Elasto-Aerodynamics-Driven Triboelectric Nanogenerator for Scavenging Air-Flow Energy

Shuhua Wang,[†,#] Xiaojing Mu,[‡,§,#] Xue Wang,[†] Alex Yuandong Gu,[‡] Zhong Lin Wang,[*,†,∥] and Ya Yang[*,†]

[†]Beijing Institute of Nanoenergy and Nanosystems, Chinese Academy of Sciences, Beijing 100083, China, [‡]Institute of Microelectronics, Agency for Science, Technology and Research (A*STAR), Singapore 117685, Singapore, [§]Defense Key Disciplines Lab of Novel Micro-nano Devices and System Technology, International R & D center of Micro-nano Systems and New Materials Technology, Key Laboratory of Optoelectronic Technology & Systems, Ministry of Education, Chongqing University, Chongqing 400044, China, and [∥]School of Materials Science and Engineering, Georgia Institute of Technology, Atlanta, Georgia 30332-0245, United States. [#]Shuhua Wang and Xiaojing Mu contributed equally.

ABSTRACT Efficient scavenging the kinetic energy from air-flow represents a promising approach for obtaining clean, sustainable electricity. Here, we report an elasto-aerodynamics-driven triboelectric nanogenerator (TENG) based on contact electrification. The reported TENG consists of a Kapton film with two Cu electrodes at each side, fixed on two ends in an acrylic fluid channel. The relationship between the TENG output power density and its fluid channel dimensions is systematically studied. TENG with a fluid channel size of 125 × 10 × 1.6 mm^3 delivers the maximum output power density of about 9 kW/m^3 under a loading resistance of 2.3 MΩ. Aero-elastic flutter effect explains the air-flow induced vibration of Kapton film well. The output power scales nearly linearly with parallel wiring of multiple TENGs. Connecting 10 TENGs in parallel gives an output power of 25 mW, which allows direct powering of a globe light. The TENG is also utilized to scavenge human breath induced air-flow energy to sustainably power a human body temperature sensor.

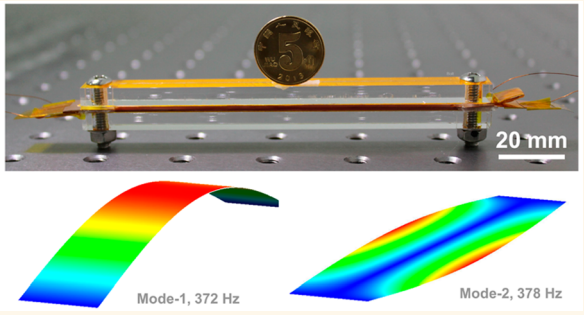

KEYWORDS: triboelectric nanogenerator · air-flow energy · aero-elastic flutter effect · temperature sensor · self-powered

Wind energy as an alternative to fossil fuels is plentiful, renewable, widely distributed, clean, and produces no greenhouse gas emissions during operation.[1,2] Due to above attributes and relatively high area energy density, it has been actively utilized, through windmill, to generate electricity in recent years. Although efficient, this centralized power generation scheme requires complex and massive power transmission and distribution system to deliver the generated electricity to the user terminals. Recent rising demands of sensor-enabled Internet of Things makes distributed power supply a must. Thus, a miniature, modularized, and efficient power generation solution is highly desired.[3−5] Due to its low cost, simple fabrication process, and good scalability, triboelectric nanogenerators (TENGs) exhibits great potential as a wind energy harvester.[6−8] TENGs scavenge mechanical energy through the coupled triboelectric and electrostatic induction effects.[9−11] Mechanically, several phenomena give rise to the dynamic response of structures under wind loading, including buffeting, vortex shedding, galloping and flutter. Of the above four phenomena, aero-elastic flutter vibrations is of great interest to this research.

Aero-elastic flutter is a "self-feeding" oscillatory motion that results from the coupling of aerodynamic forces with the elastic deformation of a structure.[12−14] Due to the result of combined bending and torsion, it is often observed in plate-like structures, such as signboards and suspension bridge decks. The instability is caused when there is a "positive feedback" between the structure's natural vibration and the aerodynamic forces. In other words, the movement of the object increases the aerodynamic load, which in turn drives the object to vibrate at a greater amplitude. The vibration levels can thus build up if the fluid energy input surpass the mechanical damping of the

* Address correspondence to yayang@binn.cas.cn, zlwang@gatech.edu.

Received for review July 16, 2015 and accepted September 5, 2015.

Published online 10.1021/acsnano.5b04396

object, which often results in large amplitudes and can lead to rapid failure. Although the flutter phenomena is normally regarded to be dangerous and destructive in rigid structures such as constructions, it also offers great opportunities for novel energy harvesting techniques employing soft materials. Although TENG has been studied intensively in recent years, a thorough simulation of aerodynamics, as well as a comprehensive system level parametric study on the effects of TENG geometries to maximize output power, is still unavailable.

In this paper, we report an elasto-aerodynamics-driven TENG characterized by underlining aero-elastic flutter phenomena. Rational design of the TENG achieves an unprecedented power density of 9 kW/m^3. The modular design of the reported TENG enables the good output power capability. The ultrahigh output power of TENG allows for direct powering of a body temperature sensor by simply harvesting human breath-induced air-flow energy. This research marks a step toward self-powered healthcare monitoring systems.

RESULTS AND DISCUSSION

Figure 1a illustrates the schematic diagram of the fabricated TENG, which includes a Kapton film with two Cu electrodes at both sides and two polytetrafluorothylene (PTFE) films with Cu electrodes at the top and bottom acrylic substrates. The Kapton film was fixed at the middle of the device by using two bolts, where two narrow air gaps were created between the PTFE films and the Kapton film. Figure 1b,c displays photographs of the TENG with the different view angles, where the device has the inner dimensions of 100 × 10 × 1.6 mm^3. The air flows into the gaps of the device and induces the vibration of the Kapton film, which can drive the working of the TENG. As depicted in Figure 1d, the dynamic process of the Kapton film under the wind speed of about 15 m/s includes three typical states, which can be also seen in the Supporting Information Movie 1. A periodic contact and separation between the Cu electrode on the Kapton film and the PTFE film under the air-flow condition can be clearly observed by using a high speed camera.

The working of the TENG is based on a periodic contact and separation between the Cu electrode on the Kapton film and the PTFE film, where the coupling between triboelectrification and electrostatic induction results in alternating flow of electrons between electrodes. As illustrated in Figure 2, the electricity generation process includes several different states. At the initial state, the Cu electrodes on the Kapton film and the PTFE films are separated by the air gaps, where there is no current/voltage output for the TENG. When the Cu electrode on the Kapton film vibrates up to get in touch with the top PTFE film under the air-flow through the TENG, the negative and positive triboelectric

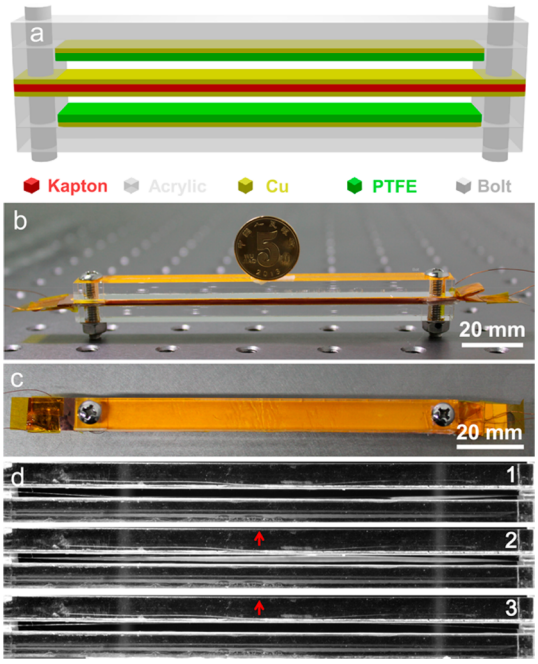

Figure 1. (a) Schematic diagram of the fabricated TENG. (b) The cross-sectional view of the fabricated TENG. (c) Top view of the fabricated TENG. (d) Photographs of TENG in motion captured by using a high-speed camera.

charges can be created on the surfaces of PTFE film and Cu electrode, respectively. When the Kapton film vibrates down to approach the bottom PTFE film, the triboelectric charges can keep on the surface of top PTFE film, while the charges on the top two Cu electrodes can flow when there is an external circuit due to the electrostatic induction of the charged PTFE film. In the vibration process of the Kapton film, both the top and bottom PTFE films have the negative triboelectric charges by rubbing the Cu electrodes. Under the strong electrostatic attraction, both the top and bottom TENGs can deliver the current/voltage signals under the air-flow condition.

Output voltage and current of TENGs in Figure 1 were measured under a wind speed of about 15 m/s. As shown in Figure 3a,b, the top TENG delivers an alternating output signals with a short-circuit current of about 80 μA and an output voltage of about 240 V under a loading resistance of 10 MΩ. The bottom TENG produces a short-circuit current of about 60 μA and an output voltage of 220 V, as displayed in Figure 3c,d. Figure 3e presents the measured output voltage under the different loading resistance, exhibiting a gradual increase with increasing the loading resistance, where the corresponding largest power density of the top TENG is about 3 kW/m^3 under the loading resistance of 2.3 MΩ. Figure 3f displays a similar change in the measured output voltage of the bottom TENG with increasing loading resistance, where the bottom TENG has the largest power density of about 2 kW/m^3. The difference of the two TENGs in one device is associated

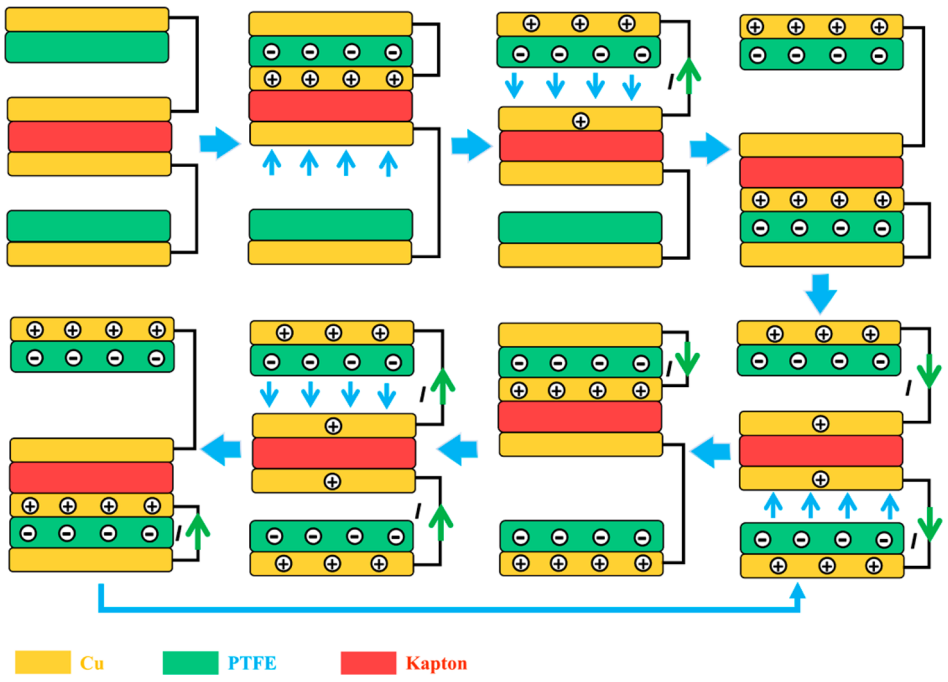

Figure 2. Schematic diagrams of the electricity generation process of TENG.

with the minor unevenness of the flexible Kapton film that can result in the different distances between the Kapton film and the top/bottom PTFE film in the vibration process. Figure S1 illustrates the charging curves of a 10 μF capacitor by using the TENG 1, TENG 2, and the TENG 1//TENG 2, indicating that the integrated TENGs can deliver a better charging performance than that of the individual TENG.

To understand the wind flutter effect in this study, the interaction behavior between the air-flow and Kapton film is qualitatively predicted by COMSOL, where the Kapton film has the size of 10 cm $\times$ 1 cm $\times$ 50 μm and is clamped on both short edges. The inlet maximum wind velocities are set to 5, 10, and 15 m/s, respectively, and the outlet pressure is set to zero as the reference pressure (Figure 4). This is a structure-fluid flow interaction model. The fluid is air with a density ρ = 1.225 kg/m^3 and dynamic viscosity η = 1.983 $\times$ 10^{-5} Pa·s. The belt structure is made of flexible material Kapton with a density ρ = 1420 kg/m^3, a Young's modulus E = 2.5 $\times$ 10^9 Pa and the Poisson's ratio ν = 0.34. The model consists of a fluid part (considered to be Newtonian and incompressible), solved with the Navier–Stokes equations in the flow channel, and the solid mechanics part (assumed to be elastic and compressible), from which a belt structural deformation is solved for using an elastic formulation and a nonlinear geometry formulation to allow large deformation. For the solid mechanics part, the short edges of the belt are fixed to the wall of the fluid channel that is oriented perpendicular to the fluid flow streamline. All other boundaries of the belt structure experience the load from the fluid. At the mean time, the outflow surface of the fluid channel is set to a zero pressure. The rest four surfaces of the fluid channel are defined as "no slip" condition, which means these surfaces serve like walls that confine the fluid flow between them.

As depicted in Figure 3a–c, the maximum deformation of the Kapton film at different inlet wind speeds were simulated, indicating that the Kapton film is mainly working at bending mode. Moreover, the corresponding pressure and the wind flow velocity distributions in the TENG under the wind speed of 15 m/s are illustrated in Figure 3, panels d and e, respectively. We found that the film deformation values are similar when the wind speed exceeds 10 m/s, suggesting that the Kapton film works at a stable state (up and down bending vibration) once the inlet wind speed approaches a specific value. On the other hands, a more interesting phenomenon can be observed that at the low inlet wind speed (5 m/s), the leading edge area of the thin film deforms larger than that of the trailing edge, resulting in the twist (torsion) motion of the film but not the bending motion. The deformation in this condition is 5 times smaller than that of the stable state at large wind speed. Normally, such small amplitude twist motion contributes less to the electric charge generation, whereas it produces attack angle of wind, which is the requirement condition of flutter occurrence. Once the inlet wind speed approaches the critical wind velocity of the Kapton thin film, the damping ratio of the twist motion will be decreased to zero and thus start the fluttering of the Kapton film. The flutter phenomenon enables the vibrated film extracting energy from the free wind flow when there

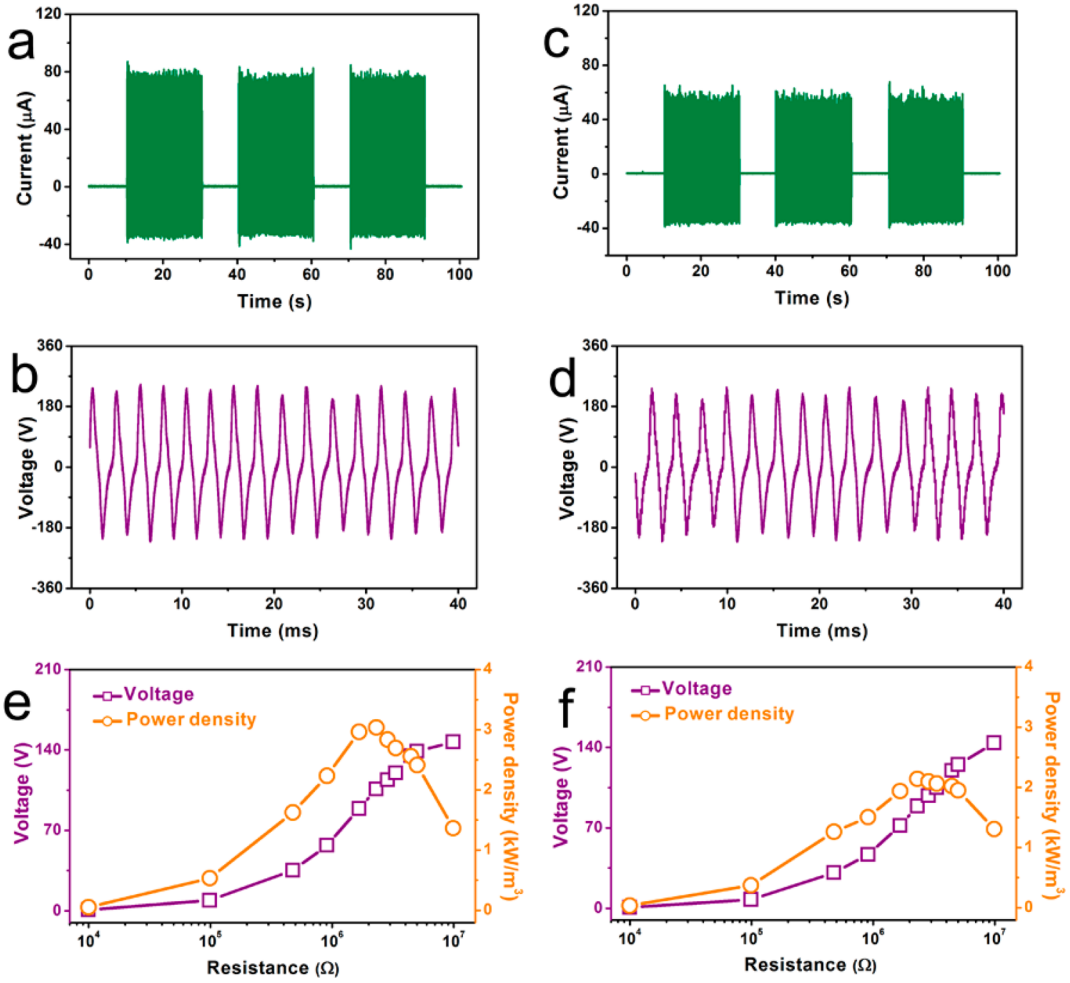

Figure 3. (a) Measured short-circuit current of TENG 1. (b) Measured output voltage of the TENG 1 under a loading resistance of 10 MΩ. (c) Short-circuit current of the TENG 2. (d) Measured output voltage of TENG 2 under a loading resistance of 10 MΩ. (e) Dependence of the output voltage and the power density for TENG 1 on the external loading resistance. (f) Dependence of the output voltage and the power density for TENG 2 on the external loading resistance.

is phase difference between film structure instantaneous aerodynamic force and elastic deformation. It will not occur at relative low air flow speed, while the large constant amplitude vibration occurs when it reaches critical wind velocity. This critical wind velocity can be determined by the frequency ratio of first order bending and twist mode and the respective damping ratio.[15] Since the flutter related vibration is periodical and neutrally stable at the critical wind speed or above, effective contact between the Kapton thin film and the top/bottom device surface will maintain in a huge wind speed range. The calculation results are completely consistent with the actual deformations in Figure 1d.

Flutter effect means that the air-flow induces the structure vibrating at its natural frequency. The natural frequencies and the mode shapes of first six order vibration mode were simulated by Coventorware. As illustrated in Figure 3f, the first and second order mode shape are bending and twisting (torsion) at the frequency of 372 and 378 Hz, respectively, where the two vibration modes are consistent with the actual vibrations of the Kapton film that were observed by using a high-speed camera (Supporting Information Movie 1). The necessary condition of the occurrence of the flutter is that the frequency of the same order twist mode is closely above that of the bending mode and the wind flow speed should approach or above the value of the critical wind velocity as well. It is clearly observed that the first two mode are in the range of 370−380 Hz, which aligns well with experimentally results in Figure 3c,d.

To obtain the largest output performance of TENG, a systematic measurement was performed by modulating the different dimensions of the device. As revealed in Figure 5a, the output voltage of TENG increases with and increase of the air gap (the distance between the top and bottom PTFE films), and dramatically reaches the maximum value of about 232 V, where the corresponding working frequency of the device is 379 Hz. Under the matched impendence of 2.3 MΩ, the largest output power density of 3 kW/m^3 responses to the air gap of 1.6 mm by analysis of the measured voltage

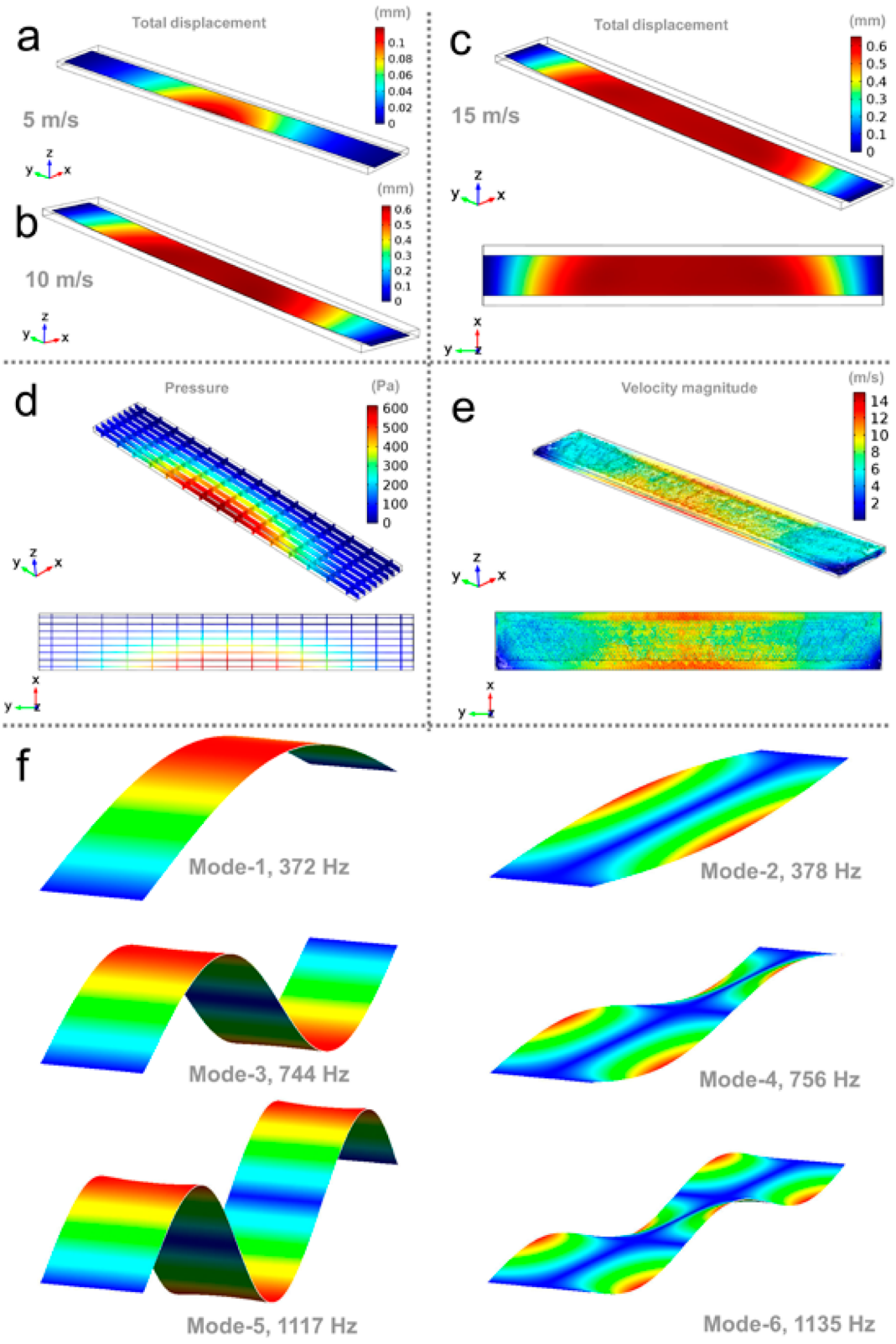

Figure 4. (a–c) Total displacement distributions of the Kapton film at the air-flow rate of 5 m/s (a), 10 m/s (b), and 15 m/s (c). (d) Pressure distribution of the Kapton film. (e) Velocity magnitude distribution of the Kapton film. (f) Different vibration modes of the Kapton film.

data under the different air gaps, as presented in Figure 5b. Figure 5c displays a dependence of the working frequency and the output voltage on the device width, showing that the working frequency of the device decreases with increasing the width of TENG and the largest output voltage is under the

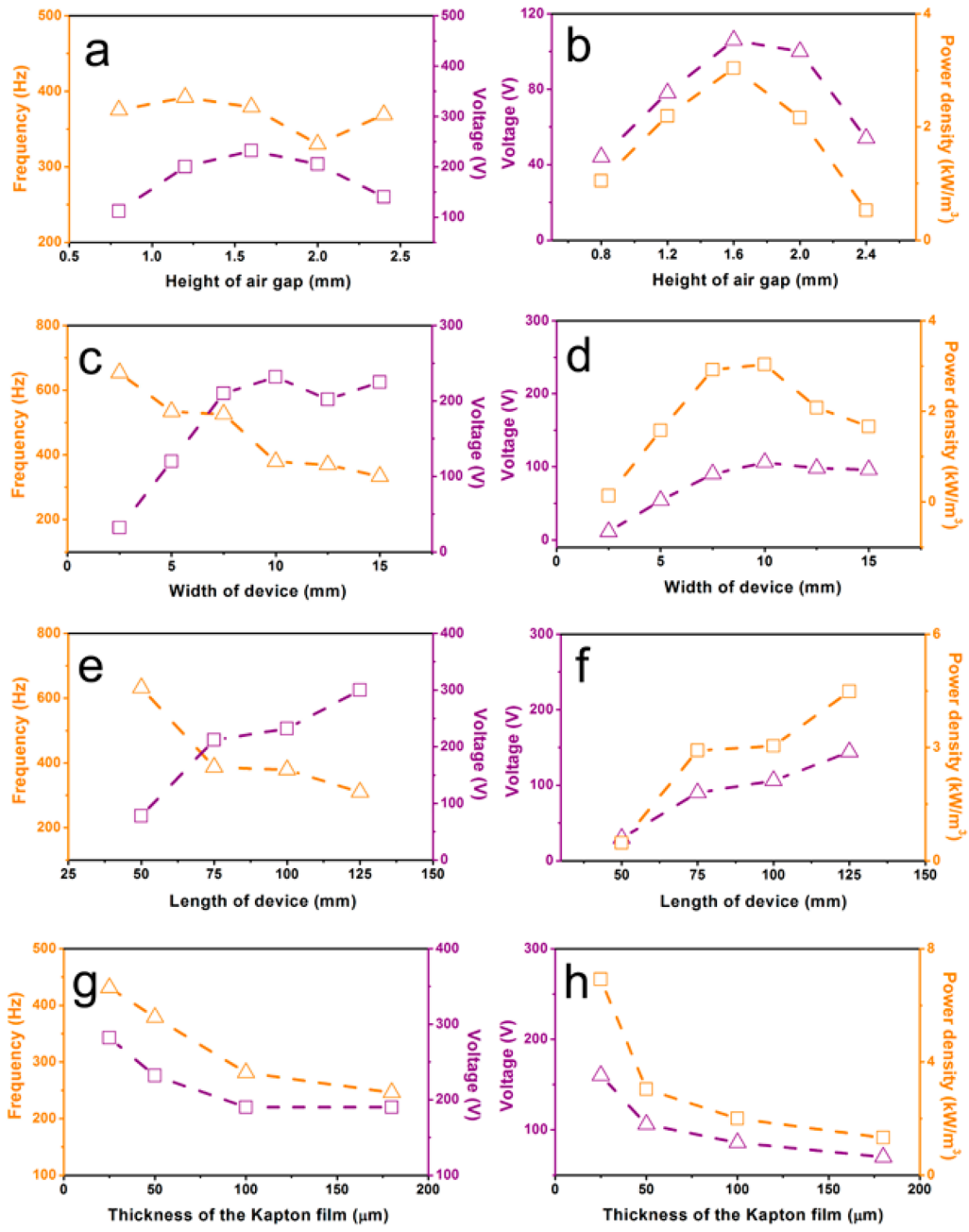

Figure 5. (a) Measured frequency and voltage of TENG under the different air gap heights. (b) Dependence of the output voltage and power density of TENG on the height of air gaps. (c) Measured frequency and voltage of TENG under the different TENG width. (d) Dependence of the output voltage and power density on the width of TENG. (e) Measured frequency and voltage of TENG under the different device length. (f) Dependence of the output voltage and power density on the length of TENG. (g) Measured frequency and voltage of TENG under the different thickness of Kapton film. (h) Dependence of the output voltage and power density on the thickness of Kapton film.

device width of 10 mm, which corresponds to a largest output power density of 3 kW/m^3, as depicted in Figure 5d. The device length can also largely influence the output performance of the TENG. As illustrated in Figure 5e,f, the working frequency of the device decreases with increasing the length of device, while the power density of TENG increases with increasing the length. In this study, a largest output power density of 4.5 kW/m^3 was achieved under the device length of about 125 mm. Panels g and h of Figure 5 exhibit the working frequency and the output power density of TENG under the different thickness of the Kapton film, respectively, indicating that the working frequency decreases with increasing the thickness of the Kapton film and the TENG has a largest output power density of 6.9 kW/m^3, where the film thickness is 25 μm. The output performance of TENG can be optimized by designing the sizes of the device, suggesting that the TENG with the dimensions of 125 $\times$ 10 $\times$ 1.6 mm^3 has the best output performance.

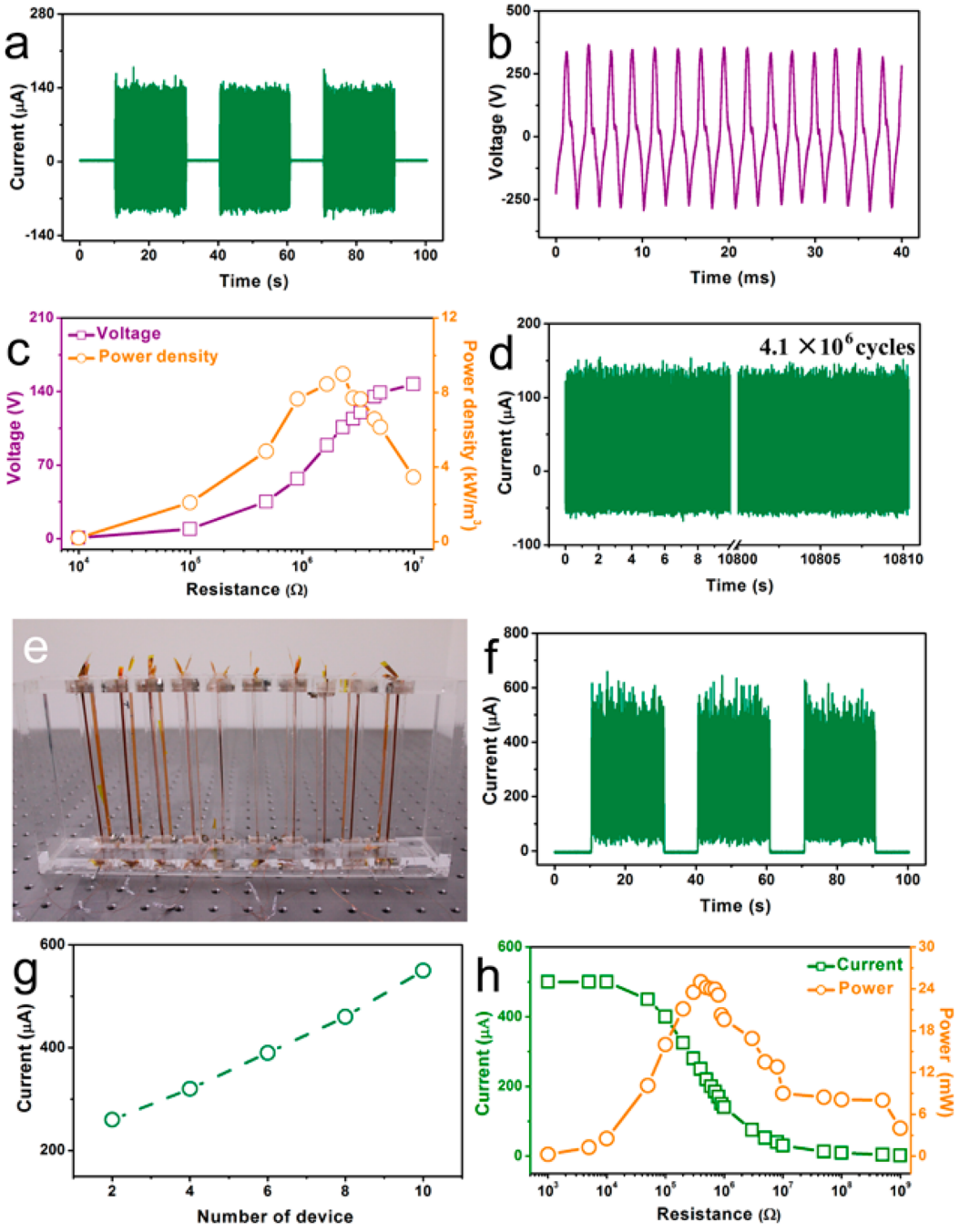

Figure 6. (a) Measured short-circuit current of the optimized TENG. (b) Measured output voltage of the optimized TENG under a loading resistance of 10 MΩ. (c) Dependence of the output voltage and power density on the external loading resistance. (d) Output current stability of the TENG under continuous working of 3 h. (e) Photograph of 10 TENGs connected in parallel. (f) Measured short-circuit current of 10 TENGs connected in parallel. (g) Scaling of the short-circuit current with different number of TENGs connected in parallel. (h) Dependence of measured output current and output power of 10 TENGs on the external loading resistance.

Operating at a wind speed of 15 m/s, the TENG with dimensions of 125 × 10 × 1.6 mm^3 can produce a short-circuit current of 140 μA and an output voltage of 342 V under the loading resistance of 10 MΩ, as displayed in Figure 6a,b. Under the matched loading resistance of 2.3 MΩ, an output power density of 9 kW/m^3 can be delivered by analysis of the output voltages of TENG under the different loading resistances, as presented in Figure 6c. As shown in Figure 6d, we also measured the reliability of TENG, indicating that there is no any change for the output current of TENG after the Kapton film vibrated to touch the PTFE film for 4.1 × 10^6 times. The lifetime of the TENG is determined by the lifetime of Cu electrode on the Kapton film under the vibration process, where the potential improvement can be achieved by improving the adhesion of Cu

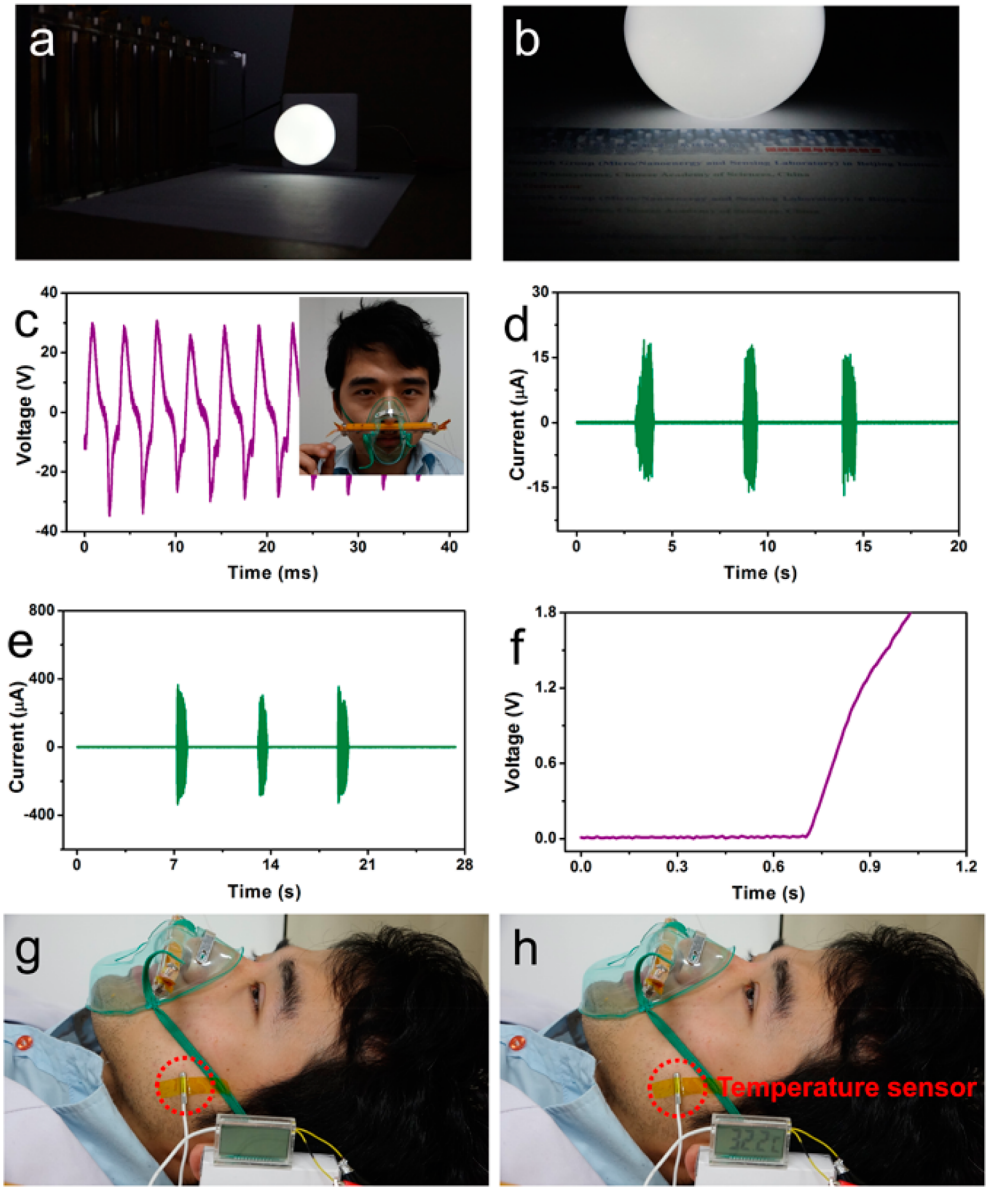

Figure 7. (a) Photograph of a spot light powered by 10 TENGs connected in parallel. (b) Photograph of a printed text on a paper illuminated by the TENGs driven spot light in complete darkness. (c and d) Measured output voltage (c) and output current (d) of the TENG for scavenging a human nose breathing induced air-flow energy. (e) Measured output current of TENG after using a transformer. (f) Measured voltage of a 10 μF capacitor charged by the TENG for scavenging a human nose breathing induced air-flow energy. (g and h) Photographs of using the TENG to scavenge human breath induced air-flow energy to sustainably power a temperature sensor system.

electrode on the Kapton film. To obtain the larger output power further, ten rectified TENGs were integrated with the connections in parallel, as displayed in Figure 6e. Figure 6f presents the output current of TENGs, showing that the total output current of 550 μA can be achieved, which is much larger than that of one device in Figure 6a. It can be found that the total output current of TENGs dramatically increases with increasing the number of device, as depicted in Figure 6g. When we measure the output current of 10 TENGs under the different loading resistances, the largest output instantaneous power of the 10 TENGs can be up to 25 mW under a loading resistance of 400 kΩ, as shown in Figure 6h. As compared with one TENG in Figure 6c, the impedance of the 10 TENGs has been largely decreased, which is beneficial for the practical applications of the TENGs as the power sources.

A transformer was utilized to increase the output current of TENG. As illustrated in Figure S2, the output current of TENG can be enhanced to be about 3.5 mA by using the transformer, while the corresponding output voltage of TENG was decreased to be about 4.4 V. The largest power density of TENG after using the transformer is about 2 kW/m^3 under a loading resistance of 2 kΩ, as displayed in Figure S2c. When 10 TENGs are integrated after using the transformers, the

total output current can be increased to 8 mA, as shown in Figure S2e. Moreover, the total output current can be increased linearly with increasing the TENG number, as depicted in Figure S2f.

To demonstrate the capability of the TENG as a power source, tens of TENGs in parallel using the rectification circuits were connected to a globe light without using a Li-on battery. Under a wind speed of 15 m/s, the white globe light can be directly driven by the TENGs (Figure 7a, Supporting Information Movie 2). Moreover, the TENGs-driven globe light can provide sufficient light intensity of about 43 lx (Figure S3) for reading printed text in complete darkness, as presented in Figure 7b (Supporting Information Movie 3).

To demonstrate that the TENG has the potential applications in self-powered healthcare monitoring, a human nose breath induced low air-flow can be used to drive the working of TENG, as shown in the inset of Figure 7c. As illustrated in Figure 7c,d, the corresponding output current and voltage can be up to 30 V and 18 μA under a loading resistance of 2.3 MΩ, respectively, resulting in an output power of 0.75 mW. As shown in Figure 7e, the output current of the TENG after using a transformer can be increased to 350 μA under a loading resistance of 4 kΩ, where the corresponding output power is about 0.49 mW. A capacitor of 10 μF can be charged from 0 to 1.8 V in 0.33 s by using the human nose breath-driven TENG, as depicted in Figure 7f. A self-powered temperature sensor system for monitoring the temperature of human body has been realized by integrating the TENG near human nose. The temperature sensor can sustainably work by using the human nose blowing induced low air-flow driven TENG, as displayed in Figures. 7g,h (Supporting Information Movie 4).

As compared with the conventional wind generation technology, the invented TENG in this study has the following advantages: (1) The conventional wind generator uses the electromagnetic effect to extract wind power, which usually requires a high cost for the device materials and installation. The TENG has very low investment cost by using the cheap organic film materials and conductive electrodes. (2) Due to the large volume, the conventional wind generators are often located in remote locations, far from cities where the transmission lines must be built to transfer the electricity from wind farm to the city. In comparison, the TENG has a very small volume so that it is suitable for TENG installation in the city such as on the house roofs and windows, where the produced electricity can be directly used by the customers. (3) The volume power density of conventional wind generator is smaller than 500 W/m^3, while the TENG has the much larger volume power density of 9 kW/m^3 under a wind speed of 15 m/s.

CONCLUSIONS

In summary, we demonstrated an elasto-aerodynamics-driven TENG for scavenging air-flow energy, where the flutter effect was employed to induce the periodic contact and separation between two triboelectric materials to realize the output of the device. By designing the different dimensions, the output performance of TENG has been optimized, where the maximum output power density of about 9 kW/m^3 has been achieved under a device working size of 125 $\times$ 10 $\times$ 1.6 mm^3. Potential large-scale air-flow energy can also be demonstrated by parallel connecting more TENGs for powering some electric devices such as a globe light. Moreover, the fabricated TENG can be utilized to harvest a human breath induced low air-flow energy to sustainably power a temperature sensor system for realizing the healthcare monitoring on human body. The TENG has the potential applications for achieving large-scale wind energy harvesting at low cost and self-powered sensor systems.

EXPERIMENTAL SECTION

Fabrication of the TENG. The fabricated device consists of two TENGs, where a TENG consists of a Kapton film with Cu electrode on its surface and a PTFE film with Cu electrode on its surface. The working of TENG is based on the air-flow induced contact and separation between two different triboelectric materials. Two acrylic sheets as the substrates of the PTFE/Cu films were cut by using a laser cutting machine. Two holes with a diameter of 5 mm were fabricated at both ends of the acrylic sheets. The supporting beams were fixed between two acrylic sheets. Screws were used to affix the two ends of the Kapton film onto the supporting beam, resulting in the Kapton film being in the middle of the TENG. When the wind flowed into the device, the Kapton film can vibrate up and down to contact the PTFE films. The periodic contact and separation between the Cu electrode on the Kapton film and the PTFE film can produce the observed voltage and current signals.

Measurement of the Fabricated Device. The output current signals of the TENG were measured by a low-noise current preamplifier (Stanford Reserch SR570). The output voltage signals of the TENG were performed by a digital phosphor oscilloscope with an internal resistance of 10 MΩ. Moreover, the vibration frequencies of the Kapton film in the device were obtained by the analysis of the output voltage signals. The dynamic vibration process of the Kapton film was performed by a high-speed camera (Phantom, v711).

Conflict of Interest: The authors declare no competing financial interest.

Acknowledgment. This work was supported by Beijing Natural Science Foundation (2154059), the National Natural Science Foundation of China (Grant No. 51472055, Grant No. 61404034), External Cooperation Program of BIC, Chinese Academy of Sciences (Grant No. 121411KYS820150028), the "thousands talents" program for the pioneer researcher and his innovation team, China. One patent has been filed based on the research presented here. Prof. Ya Yang initiated, designed, and supervised the project. Prof. Ya Yang, Prof. Zhong Lin Wang and Shuhua Wang designed the TENGs. Prof. Ya Yang and Shuhua Wang carried out the experiments, as well as the manuscript

preparation. Dr. Xiaojing Mu and Prof. Alex Yuandong Gu carried out the theoretical simulation investigation part.

Supporting Information Available: The Supporting Information is available free of charge on the ACS Publications website at DOI: 10.1021/acsnano.5b04396.

The dynamic process of TENG scavenging air-flow energy (AVI)
Scaling of TENGs for directly powering a globe light (AVI)
Scaling of TENGs for powering a globe light to provide illumination on a printed text (AVI)
Harvesting human breath induced air-flow energy to sustainably power a temperature sensor (AVI)
Measured charging voltage curves of a 10 μF capacitor, scaling of TENGs after using a transformer, measured illumination intensity of the spot light driven by 10 TENGs (PDF)

REFERENCES AND NOTES

1. Knight, J. Urban Wind Power: Breezing into Town. *Nature* **2004**, *430*, 12–13.
2. Zhou, Y.; Luckow, P.; Simith, S. J.; Clarke, L. Evaluation of Global Onshoe Wind Energy Potential and Generation Costs. *Environ. Sci. Technol.* **2012**, *46*, 7857–7864.
3. Tapia, A.; Tapia, G.; Ostolaza, J. X.; Saenz, J. R. Modeling and Control of a Wind Turbine Driven Doubly Fed Induction Generator. *IEEE Trans. Energy Convers.* **2003**, *18*, 194–204.
4. Bressers, S.; Avirovik, D.; Vernieri, C.; Regan, J.; Chappell, S.; Hotze, M.; Luhman, S.; Lallart, M.; Inman, D.; Priya, S. Small-Scale Modular Windmill. *Am. Ceram. Soc. Bull.* **2010**, *89*, 34–40.
5. Myers, R.; Vickers, M.; Kim, H.; Priya, S. Small Scale Windmill. *Appl. Phys. Lett.* **2007**, *90*, 054106.
6. Xie, Y.; Wang, S.; Lin, L.; Jing, Q.; Lin, Z.-H.; Niu, S.; Wu, Z.; Wang, Z. L. Rotary Triboelectric Nanogenerator Based on a Hybridized Mechanism for Harvesting Wind Energy. *ACS Nano* **2013**, *7*, 7119–7125.
7. Bae, J.; Lee, J.; Kim, S.; Ha, J.; Lee, B.-S.; Park, Y.; Choong, C.; Kim, J.-B.; Wang, Z. L.; Kim, H.-Y.; et al. Flutter-Driven Triboelectrification for Harvesting Wind Energy. *Nat. Commun.* **2014**, *5*, 4929.
8. Guo, H.; Chen, J.; Tian, L.; Leng, Q.; Xi, Y.; Hu, C. Airflow-Induced Triboelectric Nanogenerator as a Self-Powered Sensor for Detecting Humidity and Airflow Rate. *ACS Appl. Mater. Interfaces* **2014**, *6*, 17184–17189.
9. Fan, F.-R.; Tian, Z.-Q.; Wang, Z. L. Flexible Triboelectric Generator. *Nano Energy* **2012**, *1*, 328–334.
10. Wang, Z. L. Triboelectric Nanogenerators as New Energy Technology for Self-Powered Systems and as Active Mechanical and Chemical Sensors. *ACS Nano* **2013**, *7*, 9533–9557.
11. Zhang, X.-S.; Han, M.-D.; Meng, B.; Zhang, H.-X. High Performance Triboelectric Nanognenerators Based on Large-Scle Mass-Fabrication Technologies. *Nano Energy* **2015**, *11*, 304–322.
12. Argentina, M.; Mahadevan, L. Fluid-Flow-Induced Flutter of a Flag. *Proc. Natl. Acad. Sci. U. S. A.* **2005**, *102*, 1829–1834.
13. Bryant, M.; Wolff, E.; Garcia, E. Aeroelastic Flutter Energy Harvester Design: the Sensitivity of the Driving Instability to System Parameters. *Smart Mater. Struct.* **2011**, *20*, 125017.
14. Li, S.; Yuan, J.; Lipson, H. Ambient Wind Energy Harvesting Using Cross-Flow Fluttering. *J. Appl. Phys.* **2011**, *109*, 026104.
15. Scanlan, R. H. The Action of Flexible Bridges Under Wind, I: Flutter Theory. *J. Sound Vib.* **1978**, *60*, 187–199.